

Two-point resistances in Archimedean resistor networks

Frederic Perrier, Frédéric Girault

▶ **To cite this version:**

Frederic Perrier, Frédéric Girault. Two-point resistances in Archimedean resistor networks. Results in Physics, 2022, 36, pp.105443. 10.1016/j.rinp.2022.105443 . insu-03643018

HAL Id: insu-03643018
https://insu.hal.science/insu-03643018

Submitted on 19 May 2022

HAL is a multi-disciplinary open access archive for the deposit and dissemination of scientific research documents, whether they are published or not. The documents may come from teaching and research institutions in France or abroad, or from public or private research centers.

L'archive ouverte pluridisciplinaire **HAL**, est destinée au dépôt et à la diffusion de documents scientifiques de niveau recherche, publiés ou non, émanant des établissements d'enseignement et de recherche français ou étrangers, des laboratoires publics ou privés.



Distributed under a Creative Commons Attribution - NonCommercial - NoDerivatives 4.0 International License

Results in Physics 36 (2022) 105443

Contents lists available at ScienceDirect

Results in Physics

journal homepage: www.elsevier.com/locate/rinp

Two-point resistances in Archimedean resistor networks

Frédéric Perrier [*,1], Frédéric Girault [2]

Université Paris Cité, Institut de Physique du Globe de Paris, CNRS, F-75005 Paris, France

ARTICLE INFO

Keywords:
Resistive networks
Two-point resistance
Regular polytopes
Rotational invariance
Van Steenwijk's method

ABSTRACT

The rise of novel materials such as graphene compounds or carbon nanotubes recently revived the interest on the role of symmetries upon electrical properties. Among possible solids, symmetrical polytopes, widely realized in natural and artificial matter, deserve particular attention. When equal resistors are attached between neighbouring nodes of Perfect (Platonic) solids (PS) along the edges, the two-point resistance between any pair of nodes was established in the 1990s by van Steenwijk using an elegant and efficient method. Using van Steenwijk's method, Moddy and Aravind subsequently derived the resistance values for two Archimedean and two Catalan solids. Here, with the same method, we derive the exact expression for the two-point resistance between any two nodes for resistor networks made of equal resistors placed along the edges of the thirteen Archimedean solids (AS). While the calculation remains elementary for the simplest AS, a dedicated method using computer assistance was developed for the Snub Cube, the Snub Dodecahedron and the three AS with three different rotation symmetries (the Great Rhombicuboctahedron, the Small Rhombicosidodecahedron and the Great Rhombicosidodecahedron). The largest resistance value (191/90) is obtained between the two opposite nodes of the Truncated Dodecahedron, and the second largest (42815/21114) is obtained between the two opposite nodes of the Great Rhombicosidodecahedron. The smallest resistance value (14137/38016) is obtained between some of the neighbouring nodes of the Snub Cube, whereas the resistance between neighbouring nodes of the Icosahedron (11/30) is slightly smaller. Some general symmetry relations between two-point resistances in AS networks are also derived, as well as some relations with two-point resistances in PS networks. The complete set of exact two-point resistance values for PS and AS networks can be used to check numerical codes or to evaluate the capacity of regular solids to provide appropriate models for given experimental situations.

Introduction

Resistor networks have raised the interest of physicists since the early days of electromagnetic theory, and the rules of current conservation and electric potential closure along a loop were established by Kirchhoff by the middle of the 19th century [1]. Before the end of the 19th century, Kennelly's theorem (star-triangle or Y-Δ transform) [2], which allowed complex resistor networks to be approached elegantly, also provided the basic algorithm in computer codes for the calculation of resistance by node elimination.

The interest in basic resistor network, however, was revived considerably at the end of the 20th century and the beginning of the 21st century with the development of novel conductive materials such as fullerenes [3,4], graphene [5,6] and carbon nanotubes [7]. During the same period, van Steenwijk proposed a simple method to obtain, in networks with extensive symmetries, all values of the resistance between two nodes (two-point resistances) from the calculation of a minimum number of basic current configurations; as an example of application, he gave exact expressions for all two-point resistance values in networks based on Platonic (Perfect) solids (PS), with all edges carrying equal resistors [8]. Using van Steenwijk's method (VSM), the two-point resistance values were derived by Moody and Aravind for two Archimedean solids (AS), i.e. the Cuboctahedron and the Icosidodecahedron, and two Catalan solids, i.e. the Rhombic Dodecahedron and the Rhombic Triacontahedron [9]. However, most of the research inspired by the development of material science [3–7] focused on two-dimensional and three-dimensional resistor networks [8–9]. New theoretical methods were developed, using Green functions [10–12] or Laplacian matrix, reformulated recently as a now widely used recursion-transform [13–15].

* Corresponding author.
E-mail address: perrier@ipgp.fr (F. Perrier).
[1] ORCID: 0000-0002-6306-7478.
[2] ORCID: 0000-0001-8470-1792.

https://doi.org/10.1016/j.rinp.2022.105443
Received 20 February 2022; Accepted 19 March 2022
Available online 23 March 2022
2211-3797/© 2022 The Author(s). Published by Elsevier B.V. This is an open access article under the CC BY-NC-ND license (http://creativecommons.org/licenses/by-nc-nd/4.0/).

Recently, the general consequences of basic symmetries of resistor networks received attention, and relations between various resistance values around grid corners [16] or nodes with rotation invariance [17] were derived using elementary methods, combining Kennelly's theorem and VSM. Similarly, recurrence relations could be obtained for networks with threefold axial symmetry and repeated patterns along the axis [18], or as a function of the order of rotation in a network with an axis of symmetry [19].

AS, which already had raised the interest of Johannes Kepler in the 17th century [20], deserve some further attention [21–24]. Fullerene compounds [3,25], which show some forms as an AS solid, first synthetized in the laboratory, were subsequently found in space [4]. Faujasite, a tectosilicate zeolite crystal discovered in minerals as early as the 19th century, also has a basic AS cell [26]. Therefore, in this paper, we return to basic symmetrical AS compounds and provide exact expressions for the two-point resistance between any two nodes for the complete set of the thirteen AS networks. These networks are obtained when equal resistors are placed on all edges of the considered AS. First, we recall the basic properties of AS and we introduce the VSM, illustrated with the simple case of the Cuboctahedron [9]. For most AS, the VSM method can be handled without difficulty, and we illustrate two such examples: the Truncated Tetrahedron (TT) and the Truncated Cube (TC). For the AS with larger numbers of nodes, the calculations become heavy, and, rather, we apply the VSM method using computer assistance, a process illustrated with the cases of the Snub Cube (SC) and the Snub Dodecahedron (SD). Exact expressions of all two-point resistances for all AS networks are given and discussed in details. Finally, we show how relations between two-point resistances in AS networks and relations between selected two-point resistances in AS and PS networks can be derived from Kennelly's transforms and corner theorems [16].

Archimedean networks and van Steenwijk's method

The PS are the five regular convex polyhedrons made of identical polygonal faces. They are defined (Table 1) by their number of nodes (or vertices) V, the number of edges E and the number of faces F, satisfying Euler's relation $V-E+F=2$. The AS are the thirteen regular uniform polyhedrons composed of regular polygons having identical nodes [27]. Here, the Pseudorhombicuboctahedron, the prisms and antiprisms are not included among the AS [28]. Their parameters and their names, as used thereinafter, are given in Table 2, and they also satisfy Euler's relation, like any polygonal covering of the sphere.

AS networks (Figs. 1 and 2) are constructed by placing an identical resistor, taken as a unity resistor without loss of generality, on all edges. Here, the term AS network refers to spherical networks based on the AS solids, and does not include the Archimedean connectivity pattern referred to in two-dimensional networks [10]. The number of resistors is comparatively large for most of these networks. Only the TT and the CO (Fig. 1), with 18 and 24 resistors, respectively, have less resistors than the PS networks, which have a maximum of 30 resistors in the I and D networks. The largest number of resistors (180) is found in GRCD network (Fig. 2). The nodes are labelled from 0 to $V-1$ according to the convention shown in Figs. 1 and 2. The equivalent resistance between nodes i and j (two-point resistance) is noted R_{ij} or $R_{i,j}$ when a confusion is possible with the digits of i and j. Since all nodes are equivalent in the considered networks, we only need to calculate R_{0i}, with $0\leq i\leq V-1$.

Following Moody and Aravind [9], to compute the resistances R_{0i}, we use VSM [8]. In this method, to find the equivalent resistance between any pair of nodes, we first solve the current distribution for only a reduced number of configurations, one for each type of nodes. In our case, a single configuration is sufficient, as all nodes are equivalent. This configuration, referred to, in the following, as the base configuration, is obtained when a unity current is injected at node 0 and equal currents of $1/(V-1)$ value are recuperated at all of the $V-1$ other nodes. To find the current distribution for injection from node 0 to node i, it is sufficient to subtract, from the base configuration, the same current configuration but rotated to represent injection at node i. Summing these two configurations, the ingoing or outgoing current is zero at all nodes, except at the injection node 0 and at the extraction node i, where it is $1+1/(V-1)$. The equivalent resistance is then the sum of the obtained potential differences divided by the total current $V/(V-1)$. Since the nodes are here equivalent, the sum of the total potential drop is simply twice the total potential drop from 0 to i in the base configuration. Let us illustrate this process with the particularly simple case of the CO [9].

The base configuration for the CO network (Fig. 3) is obtained when a unity current is injected at node 0 and 1/11 is extracted from all other nodes ($V=12$). In the CO, there are two perpendicular planes of symmetry crossing at every node. Thus, the currents flowing in the four legs from node 0 are equal to 1/4. Also, because of the same planar symmetry, nodes 1 and 5, 6 and 10, 4 and 3, and 7 and 8 are equipotential. Current conservation alone is not sufficient to give the values of other currents, and one unknown current α from node 1 to node 2 is introduced (Fig. 3), equal to the current from node 3 to node 2 by symmetry. Now, current conservation gives the current from node 1 to node 6, namely $1/4-\alpha-1/11$, and from node 2 to node 6, namely $\alpha-1/22$. Incidentally, the current from node 6 to node 11 is now 1/44, and, summing the four legs going to node 11, we indeed get a total current 1/11 flowing out of node 11. As all currents in loop 1-2-6 are now expressed, we get, from Kirchhoff's law (total potential drop along a closed loop is zero), the constraint:

$$\alpha+\left(\alpha-\frac{1}{22}\right)-\left(\frac{1}{4}-\alpha-\frac{1}{11}\right)=0, \tag{1}$$

giving $\alpha=3/44$, and we infer the equivalent resistances:

Table 1
Summary of two-point resistances in Platonic (Perfect or PS) networks with edges carrying equal unity resistors. The number of faces (F), edges (E) and nodes (V) are given. N_R is the number of different values for the two-point resistance, $R_{\min}$ the smallest value, $R_{\max}$ the largest and R_a the average value. The two-point resistances are ordered according to the number of resistors between the considered nodes.

PS network	F	E	V	N_R	$R_{\min}$	$R_{\max}$	Two-point resistances	R_a
Tetrahedron (T)	4	6	4	1	$\frac{1}{2}=0.5$	$\frac{1}{2}=0.5$	$\frac{1}{2}$	0.5
Octahedron (O)	8	12	6	2	$\frac{5}{12}\cong 0.417$	$\frac{1}{2}=0.5$	$\frac{5}{12},\frac{1}{2}$	0.433 ± 0.009
Cube (C)	6	12	8	3	$\frac{7}{12}\cong 0.583$	$\frac{5}{6}\cong 0.833$	$\frac{7}{12},\frac{3}{4},\frac{5}{6}$	0.690 ± 0.019
Icosahedron (I)	20	30	12	3	$\frac{11}{30}\cong 0.367$	$\frac{1}{2}=0.5$	$\frac{11}{30},\frac{7}{15},\frac{1}{2}$	0.424 ± 0.007
Dodecahedron (D)	12	30	20	5	$\frac{19}{30}\cong 0.633$	$\frac{7}{6}\cong 1.167$	$\frac{19}{30},\frac{9}{10},\frac{16}{15},\frac{17}{15},\frac{7}{6}$	0.961 ± 0.012

Table 2
Summary of two-point resistances in Archimedean (AS) networks with edges carrying equal unity resistors. The number of faces (F), edges (E) and nodes (V) are given. N_R is the number of different values for the two-point resistance, $R_{\min}$ the smallest value, $R_{\max}$ the largest and R_a the average value.

AS network	F	E	V	N_R	$R_{\min}$	$R_{\max}$	R_a
Truncated Tetrahedron (TT)	8	18	12	5	$\frac{17}{30} \cong 0.566$	$\frac{11}{10} \cong 1.1$	0.912 ± 0.024
Truncated Octahedron (TO)	14	36	24	12	$\frac{625}{1008} \cong 0.620$	$\frac{9}{7} \cong 1.286$	1.055 ± 0.012
Truncated Icosahedron (TI)	32	90	60	23	$\frac{16273}{25080} \cong 0.649$	$\frac{17}{11} \cong 1.545$	1.296 ± 0.005
Truncated Cube (TC)	14	36	24	11	$\frac{7}{12} \cong 0.583$	$\frac{47}{30} \cong 1.567$	1.254 ± 0.017
Truncated Dodecahedron (TD)	32	90	60	23	$\frac{89}{150} \cong 0.593$	$\frac{191}{90} \cong 2.122$	1.736 ± 0.009
Small Rhombicuboctahedron (SRCO or RCO)	26	48	24	11	$\frac{767}{1680} \cong 0.457$	$\frac{57}{70} \cong 0.814$	0.682 ± 0.007
Cuboctahedron (CO)	14	24	12	4	$\frac{11}{24} \cong 0.458$	$\frac{2}{3} \cong 0.667$	0.561 ± 0.010
Icosidodecahedron (ID)	32	60	30	8	$\frac{29}{60} \cong 0.483$	$\frac{8}{9} \cong 0.889$	0.745 ± 0.006
Snub Cube (SC)	38	60	24	16	$\frac{14137}{38016} \cong 0.372$	$\frac{1937}{3168} \cong 0.611$	0.518 ± 0.005
Snub Dodecahedron (SD)	92	150	60	37	$\frac{8984731}{23905400} \cong 0.376$	$\frac{4614181}{5976350} \cong 0.772$	0.656 ± 0.003
Great Rhombicuboctahedron (GRCO)	26	72	48	33	$\frac{63859}{102960} \cong 0.620$	$\frac{1583}{990} \cong 1.599$	1.322 ± 0.008
Small Rhombicosidodecahedron (SRCD or RCD)	62	120	60	23	$\frac{52543}{114840} \cong 0.457$	$\frac{651}{638} \cong 1.020$	0.863 ± 0.003
Great Rhombicosidodecahedron (GRCD)	62	180	120	75	$\frac{41543021}{66878595} \cong 0.621$	$\frac{42815}{21114} \cong 2.028$	1.705 ± 0.004

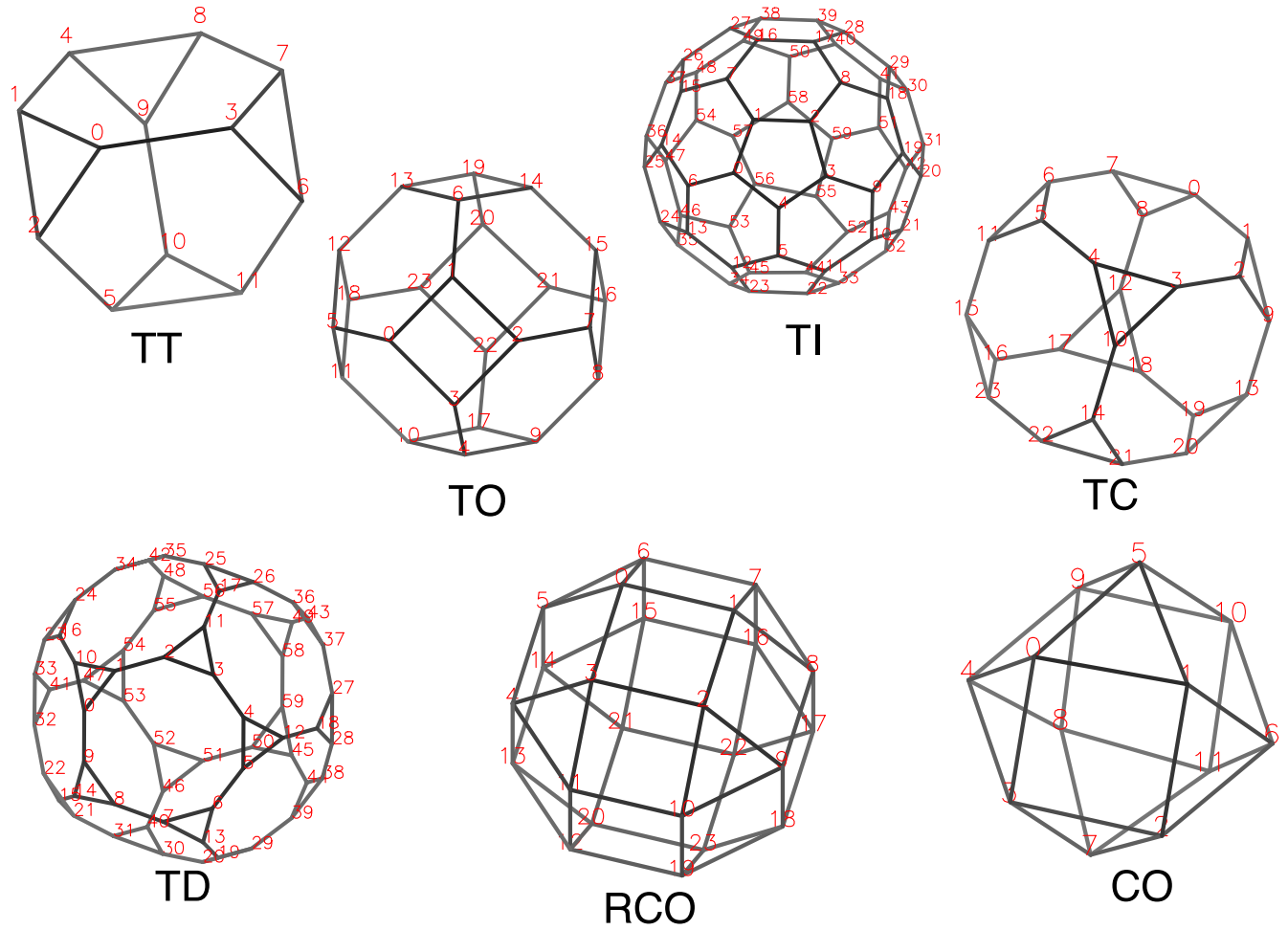


Fig. 1. First set of Archimedean networks: Truncated Tetrahedron (TT), Truncated Octahedron (TO), Truncated Icosahedron (TI), Truncated Cube (TC), Truncated Dodecahedron (TD), Small Rhombicuboctahedron (SRCO or RCO) and Cuboctahedron (CO). The numbers indicate the node labelling.

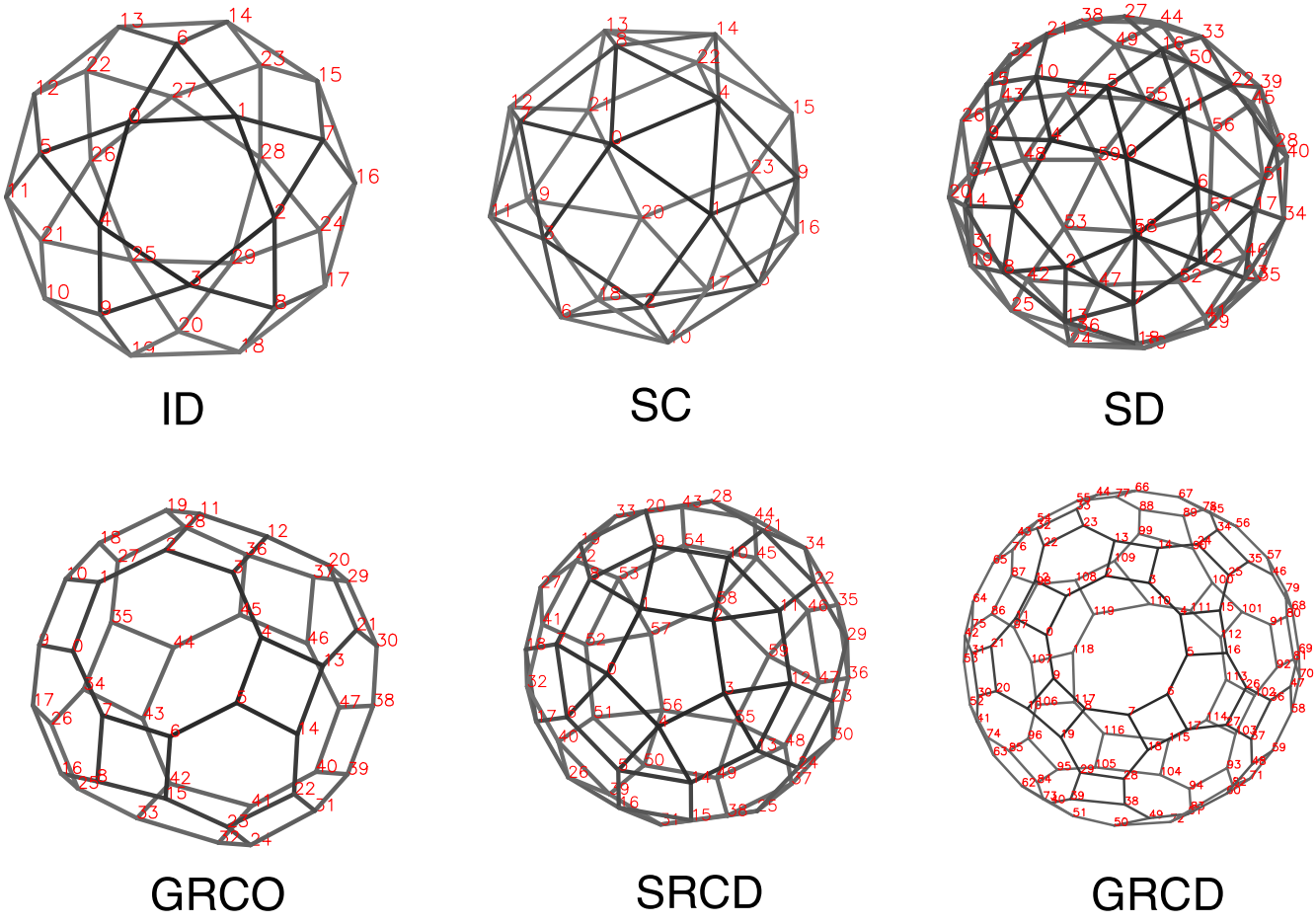


Fig. 2. Second set of Archimedean networks: Icosidodecahedron (ID), Snub Cube (SC), Snub Dodecahedron (SD), Great Rhombicuboctahedron (GRCO), Small Rhombicosidodecahedron (SRCD or RCD) and Great Rhombicosidodecahedron (GRCD).

$$\begin{cases} R_{01} = R_{03} = R_{04} = R_{05} = \frac{11}{12} 2 \frac{1}{4} = \frac{11}{24} \\ R_{02} = R_{09} = \frac{11}{12} 2 \left(\frac{1}{4} + \alpha \right) = \frac{7}{12} \\ R_{06} = R_{07} = R_{08} = R_{010} = \frac{11}{12} 2 \left(\frac{1}{4} + 2\alpha - \frac{1}{22} \right) = \frac{5}{8} \\ R_{011} = R_{09} = \frac{11}{12} 2 \left(\frac{1}{4} + 2\alpha - \frac{1}{22} + \frac{1}{44} \right) = \frac{2}{3} \end{cases} . \quad (2)$$

For the AS networks, the calculations can get heavier, but the principle remains the same. First, we show two moderately complicated cases, where calculations remain feasible without considerable efforts.

Two-point resistances in the simplest Archimedean networks

The case of the TT network, which has 12 nodes like the CO network, remains relatively easy (Fig. 4). In this case, there is only one plane of symmetry at each node, which corresponds to a bisecting plane of the network carried by nodes 0 and 3. Thus, in the base configuration, nodes 1 and 2, 6 and 7, 9 and 10 are equipotential. One unknown current α needs to be introduced from node 0 to node 1, equal by symmetry to the current from node 0 to node 2, and the current from node 0 to node 3 consequently is 1–2α. From current conservation, the currents from node 3 to node 6, from node 6 to node 11 and from node 2 to node 5 (Fig. 4) are 1/2−α−1/22, 1/2−α−3/22 and α−1/11, respectively. To continue the determination of currents, we proceed using current conservation and introduce new unknowns only when current conservation is not sufficient. Here, therefore, we introduce an unknown current β from node 5 to node 10, which gives a current $\beta-1/11$ from node 10 to node 11 (Fig. 4). Using the closed loop 5-10-11, the current from node 5 to node 11 also follows, equal to $2\beta-1/11$. Current conservation at node 5 imposes:

$$\alpha - \frac{1}{11} = \beta + \left(2\beta - \frac{1}{11} \right) + \frac{1}{11}, \quad (3)$$

while the closed loop 0-2-5-11-6-3 gives:

$$\alpha + \left(\alpha - \frac{1}{11} \right) + \left(2\beta - \frac{1}{11} \right) - \left(\frac{1}{2} - \alpha - \frac{3}{22} \right) - \left(\frac{1}{2} - \alpha - \frac{1}{22} \right) - (1 - 2\alpha) = 0, \quad (4)$$

and we obtain:

$$\begin{cases} \alpha - 3\beta = \dfrac{1}{11}, \\ 3\alpha + \beta = 1 \end{cases} \tag{5}$$

hence α=17/55 and β=4/55. Having solved the base configuration, we obtain the equivalent resistances:

$$\begin{cases} R_{01} = R_{02} = \dfrac{11}{12} 2\alpha = \dfrac{17}{30} \\ R_{03} = \dfrac{11}{12} 2(1-2\alpha) = \dfrac{7}{10} \\ R_{04} = R_{05} = \dfrac{11}{12} 2\left(2\alpha - \dfrac{1}{11}\right) = \dfrac{29}{30} \\ R_{06} = R_{07} = \dfrac{11}{12} 2\left(\dfrac{3}{2} - 3\alpha - \dfrac{1}{22}\right) = \dfrac{29}{30} = R_{04} = R_{05} \\ R_{08} = R_{011} = \dfrac{11}{12} 2\left(2\alpha - \dfrac{1}{11} + 2\beta - \dfrac{1}{11}\right) = \dfrac{16}{15} \\ R_{010} = R_{09} = \dfrac{11}{12} 2\left(2\alpha - \dfrac{1}{11} + \beta\right) = \dfrac{11}{10} \end{cases} . \tag{6}$$

The equality between R_{06} and R_{05}, which emerged in Eqs. (6), results from the rotational symmetry of order 3 around a central axis of the TT passing through the centre of each triangular face (Fig. 4). Other equalities result from the central planar symmetries of the TT.

The case of the TC network, while slightly more difficult, is handled in the same manner, but now V=24 (Table 2) and more variables need to be introduced (Fig. 5). In this case also, there is only one plane of symmetry at each node; it corresponds to a bisecting plane of the network. For example, in the base configuration, it corresponds to the plane containing nodes 0, 1, 22 and 23 (Fig. 5). In this case, nodes in the pairs 7-8, 2-9, 14-21 and 15-16 are equipotential. As above for the TT, one unknown current α is introduced from node 0 to node 1, giving two currents 1/2−α equal by symmetry from node 0 to node 7 and from node 0 to node 8. From current conservation, the currents from node 1 to node 2, from node 2 to node 3 and from node 7 to node 6 (Fig. 5) are α/2–1/46, α/2–3/46 and 1/2– α/2–1/23, respectively.

To be able to proceed, we introduce an unknown current β from node 6 to node 5 and an unknown current γ from node 3 to node 4, which give a current 1/2−α/2−β−2/23 from node 6 to node 11 and a current α/2−γ−5/46 from node 3 to node 10 (Fig. 5). From closed loop 6-5-11, we obtain a current 1/2−α/2–2β−2/23 from node 5 to node 11, which leads, using current conservation at node 5, to a current −1/2+α/2+3β+1/23 from node 5 to node 4 and, using current conservation at node 4, to a current −1/2+α/2+3β+γ from node 4 to node 10 and, with current conservation at node 10, to a current −1/2+α+3β−7/46 from node 10 to node 14. Similarly, with current conservation at node 11, we obtain a current 1−α−3β−5/23 from node 11 to node 15. We then get a current −1/2+α+3β−9/46 from node 14 to node 22 and a current 1−α−3β−6/23 from node 15 to node 23, leading to 2–2α−6β−13/23 from node 23 to node 22. At node 22, we can check that current conservation gives:

$$\left(2 - 2\alpha - 6\beta - \frac{13}{23}\right) + 2\left(-\frac{1}{2} + \alpha + 3\beta - \frac{9}{46}\right) = 1 - \frac{22}{23} = \frac{1}{23}, \tag{7}$$

as required.

After all the currents are thus expressed in the TC base configuration (Fig. 5), we write the three constraints that have not yet been used. The closed loop 3-4-10 gives:

$$\gamma + \left(-\frac{1}{2} + \frac{1}{2}\alpha + 3\beta + \gamma\right) - \left(\frac{1}{2}\alpha - \gamma - \frac{5}{46}\right) = 0, \tag{8}$$

while the octagonal closed loops 0-1-2-3-4-5-6-7 and 4-10-14-22-23-15-11-5 give, respectively:

$$\begin{aligned} &\alpha + \left(\frac{1}{2}\alpha - \frac{1}{46}\right) + \left(\frac{1}{2}\alpha - \frac{3}{46}\right) + \gamma - \left(-\frac{1}{2} + \frac{1}{2}\alpha + 3\beta + \frac{1}{23}\right) - \\ &\beta - \left(\frac{1}{2} - \frac{1}{2}\alpha - \frac{1}{23}\right) - \left(\frac{1}{2} - \frac{1}{2}\alpha\right) = 0, \end{aligned} \tag{9}$$

and:

$$\begin{aligned} &\left(-\frac{1}{2} + \frac{1}{2}\alpha + 3\beta + \gamma\right) + \left(-\frac{1}{2} + \alpha + 3\beta - \frac{7}{46}\right) + \left(-\frac{1}{2} + \alpha + 3\beta - \frac{9}{46}\right) \\ &- \left(2 - 2\alpha - 6\beta - \frac{13}{23}\right) - \left(1 - \alpha - 3\beta - \frac{6}{23}\right) - \left(1 - \alpha - 3\beta - \frac{5}{23}\right) \\ &- \left(\frac{1}{2} - \frac{1}{2}\alpha - 2\beta - \frac{2}{23}\right) + \left(-\frac{1}{2} + \frac{1}{2}\alpha + 3\beta + \frac{1}{23}\right) = 0. \end{aligned} \tag{10}$$

Hence we obtain the system:

$$\begin{cases} \beta + \gamma = \dfrac{3}{23} \\ 5\alpha - 8\beta + 2\gamma = \dfrac{27}{23} \\ 15\alpha + 52\beta + 2\gamma = \dfrac{261}{23} \end{cases} , \tag{11}$$

giving α=9/23, β=12/115 and γ=3/115. The two-point resistances in the TC follow:

$$\begin{cases} R_{01} = \dfrac{23}{24} 2\alpha = \dfrac{3}{4} \\ R_{07} = R_{08} = \dfrac{23}{24} 2\left(\dfrac{1}{2} - \dfrac{1}{2}\alpha\right) = \dfrac{7}{12} \\ R_{02} = R_{09} = \dfrac{23}{24} 2\left(\dfrac{3}{2}\alpha - \dfrac{1}{46}\right) = \dfrac{13}{12} \\ R_{06} = R_{012} = \dfrac{23}{24} 2\left(1 - \alpha - \dfrac{1}{23}\right) = \dfrac{13}{12} = R_{02} = R_{09} \\ R_{05} = R_{018} = \dfrac{23}{24} 2\left(1 - \alpha + \beta - \dfrac{1}{23}\right) = \dfrac{77}{60} \\ R_{03} = R_{013} = \dfrac{23}{24} 2\left(2\alpha - \dfrac{2}{23}\right) = \dfrac{4}{3} \\ R_{04} = R_{019} = \dfrac{23}{24} 2\left(2\alpha + \gamma - \dfrac{2}{23}\right) = \dfrac{83}{60} \end{cases} , \tag{12}$$

and:

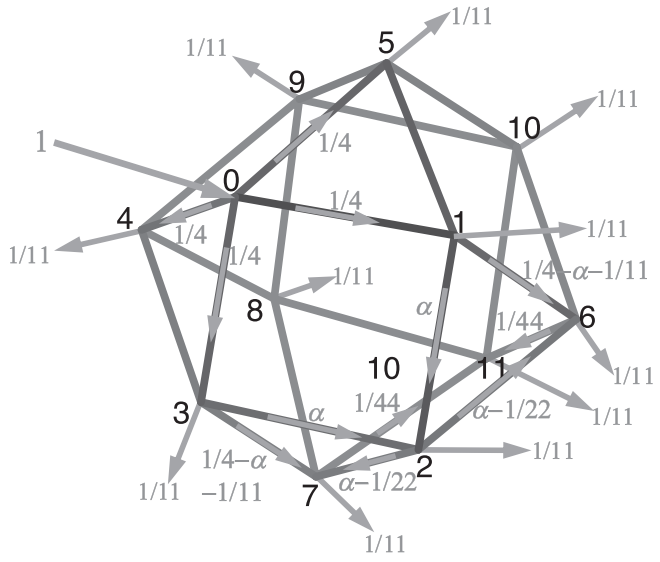


Fig. 3. Base van Steenwijk's current configuration in the Cuboctahedron (CO). One unknown current α is introduced. The currents are counted positive in the direction of the arrows.

$$\begin{cases} R_{010} = R_{020} = \frac{23}{24} 2\left(\frac{5}{2}\alpha - \gamma - \frac{9}{46}\right) = \frac{29}{20} \\ R_{011} = R_{017} = \frac{23}{24} 2\left(\frac{3}{2} - \frac{3}{2}\alpha - \beta - \frac{3}{23}\right) = \frac{13}{10} \\ R_{014} = R_{021} = \frac{23}{24} 2\left(-\frac{1}{2} + \frac{7}{2}\alpha + 3\beta - \gamma - \frac{8}{23}\right) = \frac{31}{20} \\ R_{015} = R_{016} = \frac{23}{24} 2\left(\frac{5}{2} - \frac{5}{2}\alpha - 4\beta - \frac{8}{23}\right) = \frac{29}{20} = R_{010} = R_{020} \\ R_{022} = \frac{23}{24} 2\left(-1 + \frac{9}{2}\alpha + 6\beta - \gamma - \frac{25}{46}\right) = \frac{47}{30} \\ R_{023} = \frac{23}{24} 2\left(\frac{7}{2} - \frac{7}{2}\alpha - 7\beta - \frac{14}{23}\right) = \frac{91}{60} \end{cases} . \quad (13)$$

The non-trivial equalities R_{06}=R_{02} and R_{015}=R_{010} in Eqs. (12–13) result from the four-fold rotational invariance of the TC around each axis passing through the centre of the octagonal faces. The other equalities result from the central planar symmetries.

Other AS networks, i.e. TO, TI, TD, SRCO (Fig. 1) and ID (Fig. 2), can be treated in the same manner without much difficulty, even in the case of TD which is the not the most complicated in this category, but requires 7 unknown variables. The obtained results for the two-point resistances are given in Table 3. For the remaining AS networks, i.e. the chiral networks (SC and SD) and the three AS with three different types of faces (GRCO, SRCD and GRCD), however, the calculations become difficult to perform within a reasonable amount of time and computer assistance offers a more appropriate approach.

Two-point resistances in the more complicated Archimedean networks

The method is first illustrated with the Snub Cube (Fig. 6). The number of nodes in the SC is V=24 (Table 2); therefore, in van Steenwijk's base configuration, a current of 1/23 is extracted from all nodes from 1 to V−1. In the SC, each node has multiplicity 5 and, in the base configuration (Fig. 6), four unknown currents (α, β, γ and δ) need to be introduced from node 0. Then, as shown in the previous cases, the currents are expressed using Kirchhoff's laws, and new variables are introduced when current conservation of triangle loop closure is not sufficient. After three additional unknowns are introduced (ε, μ and ν), all currents can be expressed in terms of the unknowns.

To obtain these expressions of all currents, however, computer assistance is used and coded in the form of a simple symbolic calculation. Each current is a natural integer array of dimension 9. The first component is the constant term, the second component is the term in 1/23, and the seven other components are the coefficients of the seven unknown variables. In terms of these arrays, the application of Kirchhoff's laws is a simple operation. The fact that this decomposition is not strictly speaking a mathematical base of a vector space, as the constant term and the 1/23 are not linearly independent, is of no consequence here. In contrast, it helps to follow the calculation to keep these two terms separated, as it was done in Fig. 5 for the case of the TC.

After all currents are expressed, the constraints are expressed in terms of the currents using the remaining closed loops, and the following linear system in terms of the seven unknowns is obtained:

$$\begin{cases} 535\alpha - 3860\beta + 5573\gamma - 1268\delta - 1618\varepsilon - 1006\mu - 650\upsilon = 11 + \frac{1212}{23} \\ 26\alpha - 78\beta + 172\gamma - 110\varepsilon + 15\mu - 15\upsilon = 13 + \frac{62}{23} \\ 110\alpha - 807\beta + 1146\gamma - 272\delta - 298\varepsilon - 220\mu - 146\upsilon = \frac{237}{23} \\ 68\alpha - 386\beta + 214\gamma - 146\delta + 169\varepsilon - 217\mu + 19\upsilon = -32 - \frac{104}{23} \\ 266\alpha - 1410\beta + 1792\gamma - 402\delta - 527\varepsilon - 321\mu - 93\upsilon = -2 + \frac{290}{23} \\ -220\alpha + 1352\beta - 1580\gamma + 392\delta + 172\varepsilon + 532\mu + 116\upsilon = 10 - \frac{150}{23} \\ -158\alpha + 1213\beta - 1320\gamma + 408\delta - 116\varepsilon + 633\mu + 165\upsilon = 27 - \frac{55}{23} \end{cases} , \quad (14)$$

a system that is solved exactly with a linear solver (WIMS2.24 by Gang Xiao, available online at wims.univ-cotedazur.fr, last accessed August 2019).

We obtain α=15137/(23×3168), β=1193/(23×264), δ=γ=14137/(23×3168), ε=2429/(23×1584), μ=−37/(23×1584) and ν=163/(23×264). From these values and the expressions of currents, we establish the expression of the two-resistances given in Table 4. The result δ=γ, which must be a consequence of the symmetries of the SC, was not obvious beforehand.

The two-point resistances are found in the same manner for the GRCO, which requires also seven unknowns, and for the SRCD, which is simpler and requires only five unknowns (Table 5). The cases of the SD and GRCD are the most complicated, both requiring eleven unknowns, and the case of the SD network is therefore explained to illustrate this type of solution.

The number of nodes in the SD is V=60; therefore, in van Steenwijk's base configuration (Fig. 7), a current of 1/59 is extracted from all nodes from 1 to V−1. In the SD, as in the case of the SC, each node has multiplicity 5 and, in the base configuration (Fig. 7), four unknown currents (α, β, γ and δ) need to be introduced from node 0. After seven additional unknowns are introduced (ε, μ, ν, η, ρ, ω and ξ), as shown in Fig. 7, all currents can be expressed in terms of the eleven unknowns using the same symbolic calculus as used for the SC. This time, each current is a 13-component array, with the first component being the constant term, the second component the term in 1/59, and the eleven other components the coefficients of the eleven unknown variables.

In this case, using the obtained expressions of the currents, and

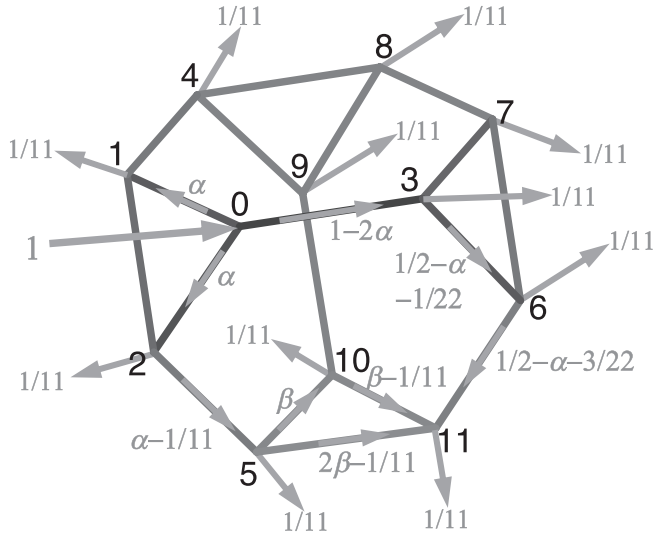


Fig. 4. Base van Steenwijk's current configuration in the Truncated Tetrahedron (TT). Two unknown current α and β are introduced. Currents are symmetric with respect to the bisecting plane carrying nodes 0 and 3. Currents given by symmetry through this plane are not drawn.

writing the remaining constraints from the closed loops not already used, the following linear system is obtained in terms of the eleven unknowns:

$$\begin{cases}
-26958\alpha + 18222\beta + 1444\gamma + 1255\delta + 42954\varepsilon + 53414\mu + 15572\upsilon - 5182\eta - 6618\rho - 2240\omega + 398\chi = 1625 - \frac{13220}{59} \\
33903\alpha + 15423\beta + 15214\gamma + 13372\delta + 50406\varepsilon - 33370\mu - 52624\upsilon + 125686\eta - 41400\rho - 398\omega + 3332\chi = 15228 + \frac{48701}{59} \\
174003\alpha + 77793\beta + 75076\gamma + 60538\delta + 290748\varepsilon - 188272\mu - 304234\upsilon - 732292\eta - 264468\rho - 3332\omega + 16778\chi = 75077 - \frac{290782}{59} \\
-1332\alpha + 3258\beta + 1018\gamma + 1207\delta + 6894\varepsilon + 4628\mu - 94\upsilon - 5164\eta - 1893\rho - 209\omega + 209\chi = 1151 + \frac{133}{59} \\
-1968\alpha - 3078\beta + 30\gamma + 690\delta + 13854\varepsilon - 5730\mu - 54594\upsilon - 20892\eta + 19212\rho - 8334\omega - 3870\chi = -588 + \frac{9366}{59} \\
168771\alpha + 70821\beta + 79782\gamma + 73170\delta + 307266\varepsilon - 186054\mu - 457560\upsilon - 713577\eta - 13791\rho - 32046\omega + 4926\chi = 77855 + \frac{277961}{59} \\
40338\alpha - 7008\beta + 8274\gamma + 7566\delta - 9966\varepsilon - 56490\mu - 36810\upsilon - 53274\eta - 10932\rho + 1254\omega + 1254\chi = 7524 + \frac{31854}{59} \\
220518\alpha - 85506\beta + 15958\gamma + 11329\delta - 159288\varepsilon - 383485\mu - 197668\upsilon - 220246\eta - 52737\rho + 11707\omega + 3059\chi = 14545 + \frac{180024}{59} \\
477132\alpha - 45624\beta + 101558\gamma + 85532\delta + 85920\varepsilon - 719405\mu - 690260\upsilon - 1032932\eta - 252600\rho - 7462\omega + 12412\chi = 97748 + \frac{534909}{59} \\
112422\alpha - 32145\beta + 13489\gamma + 9853\delta - 66741\varepsilon - 174952\mu - 61957\upsilon - 118006\eta - 47520\rho + 11065\omega + 5375\chi = 12488 + \frac{86251}{59} \\
247953\alpha + 105615\beta + 101814\gamma + 79326\delta + 391158\varepsilon - 276288\mu - 387264\upsilon - 1025451\eta - 403524\rho + 3954\omega + 26130\chi = 102437 + \frac{412817}{59}
\end{cases} \quad . \qquad (15)$$

The system Eq. (15) still can be solved exactly with the same linear solver, and we obtain α=5964797/(59×4781008), $\beta=\gamma$=26954193/(59×2390540), δ=6871376/(59×597635), ε=5580547/(59×1195270), μ=−210391/(59×1195270), ν=0, η=2098867/(59×1195270), ρ=−25677/(59×597635), ω=−84789/(59×1195270) and χ=960683/(59×1195270). From these values and the coded expressions of currents, we establish the expressions of the two-resistances given in Table 4. The results $\beta=\gamma$ and ν=0, which must be consequences of the symmetries of the SD, as in the case of the SC above, were not obvious to anticipate.

The case of the GRCD is handled in the same manner, which completes Table 5. The obtained results will now be summarized and discussed. All these exact results, expressed as rational fractions, have been checked using a standard numerical code based on node elimination by Kennelly's theorem to better than fourteen significant digits (double precision).

Results and discussion

The exact expressions of all two-point resistances in AS networks are collected in Tables 3-5 and summarized in Table 2, where the number of different resistance values N_R, the smallest value $R_{\min}$, the largest value $R_{\max}$ and the average value R_a of all two-point resistances in the network are given. These parameters are also given in Table 1 for the PS networks. The two-point resistances are summarized graphically in Fig. 8. For a given network, the two-point resistance values are shown in increasing order as a function of their occurrence fraction, which is the rank of the given node pair divided by the total number of pairs $V/(V-1)/2$. For example, in the TT network (Table 3), the value 7/10 appears 6 times among the 66 possible node pairs, hence in a fraction 1/11≅ 9% of times, while the value 29/30 appears for 24 different node pairs, hence in a fraction 24/66≅ 36% of times.

Resistance values can now be examined for the AS networks and compared with values in the PS networks. For the AS networks, the largest number of different resistance values (75) is obtained for the GRCD network, while the smallest number (4) is obtained for the CO network. The largest resistance value (191/90≅ 2.122) is obtained between the two opposite nodes of the TD network, and the second largest (42815/21114≅ 2.028) is obtained between the two opposite nodes of the GRCD network. The smallest value (14137/38016≅ 0.372) is obtained between some of the neighbouring nodes of the SC network, but the resistance between neighbouring nodes of the PS I network (11/30≅ 0.367) is smaller. In the TD network, 420 node pairs (out of 1770)

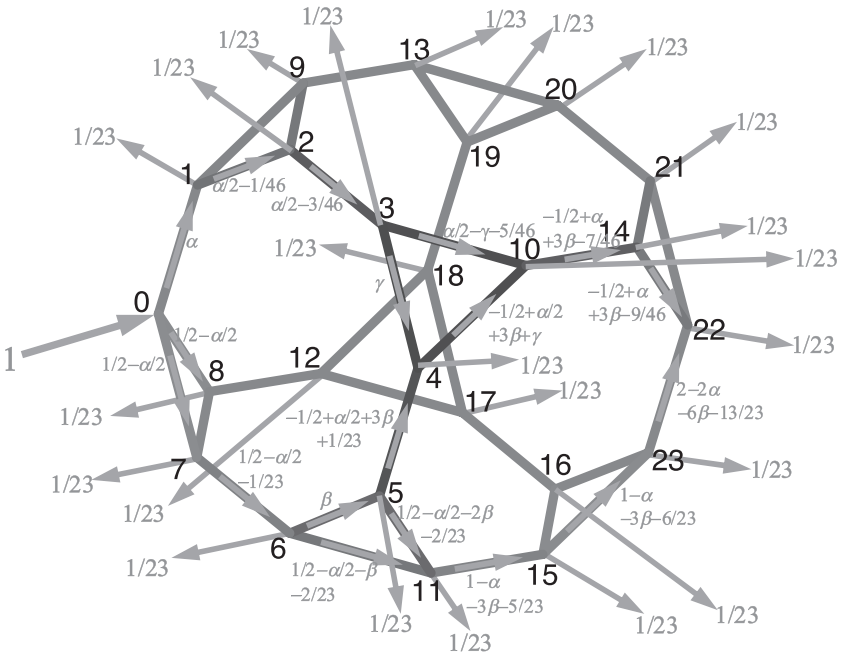


Fig. 5. Base van Steenwijk's current configuration in the Truncated Cube (TC). Three unknown currents α, β and γ are introduced. Only currents above the plane carried by nodes 0, 1, 22 and 23, located towards the reader, are drawn. The currents below this plane are given by reflection in the plane.

have a resistance larger than 2, with 7 different values (Fig. 8). In the GRCD, 600 node pairs (out of 7140) have a resistance larger than 2, with, similarly, 8 different values (Fig. 8). The smallest value in the TD network (89/150≅ 0.593) is also smaller than the smallest value (41543021/66878595≅ 0.621) in the GRCD network.

When considering the average values R_a (Table 2), the largest are again found in the TD and GRCD networks, with values of 1.736 and 1.705, respectively, but the smallest R_a value (0.518) is found in the SC network. By comparison, the average values in the PS networks (Table 1) vary from 0.433 (O) to 0.961 (D). When the dipole–dipole energy is calculated instead of the two-point resistance, the minimum interaction energy is found for the TI [29]. The symmetry of the solid, thus, has different effects depending on the considered physical property.

The relative range (RR) of resistance values, defined as the ratio R_{max}/R_{min}, shows a large dispersion as a function of the number of resistors (Fig. 9). While RR varies over a limited interval for PS networks (from 1 for the T network to ≅1.842 for the D network), it varies from ≅1.455 for the CO network to ≅3.577 for the TD network. The next largest values of RR, namely ≅3.264, ≅2.686 and ≅2.578, are obtained for the GRCD, TC and GRCO networks, respectively. For similar numbers of resistors, from 60 to 90, the values of RR vary considerably (Fig. 9), from ≅0.518 for the SC network, to the maximum RR value (3.577) of the TD network. This fact emphasizes the large changes of two-point resistances produced by apparently minor changes in the connectivity pattern of a network.

Table 3
Complete two-point resistances in the first set, displayed in Fig. 1, of Archimedean (AS) networks with edges carrying equal unity resistors. The given values correspond to the resistance between node 0 and node i, with increasing i from 1 to V−1 (see Table 2), with the convention for the numbering nodes shown in Figs. 1 and 2.

AS Network	Two-point resistance values
Truncated Tetrahedron	$\frac{17}{30}, \frac{17}{30}, \frac{7}{10}, \frac{29}{30}, \frac{29}{30}, \frac{29}{30}, \frac{29}{30}, \frac{16}{15}, \frac{11}{10}, \frac{11}{10}, \frac{16}{15}$
Truncated Octahedron	$\frac{625}{1008}, \frac{45}{56}, \frac{625}{1008}, \frac{109}{112}, \frac{341}{504}, \frac{109}{112}, \frac{137}{126}, \frac{19}{16}, \frac{1153}{1008}, \frac{1081}{1008}, \frac{109}{112}, \frac{109}{112}, \frac{1081}{1008}, \frac{1153}{1008}, \frac{19}{16}, \frac{629}{504}, \frac{19}{16}, \frac{137}{126}, \frac{19}{16}, \frac{1273}{1008}, \frac{9}{7}, \frac{1273}{1008}, \frac{69}{56}$
Truncated Icosahedron	$\frac{16273}{25080}, \frac{11617}{12540}, \frac{11617}{12540}, \frac{16273}{25080}, \frac{24749}{25080}, \frac{8389}{12540}, \frac{24749}{25080}, \frac{2669}{2280}, \frac{2669}{2280}, \frac{1312}{1045}, \frac{3733}{3135}, \frac{13637}{12540}, \frac{24749}{25080}, \frac{24749}{25080}, \frac{13637}{12540}, \frac{3733}{3135}, \frac{1312}{1045}, \frac{32519}{25080}$, $\frac{32519}{25080}, \frac{34843}{25080}, \frac{6881}{5016}, \frac{32519}{25080}, \frac{1312}{1045}, \frac{2669}{2280}, \frac{2669}{2280}, \frac{1312}{1045}, \frac{32519}{25080}, \frac{6881}{5016}, \frac{34843}{25080}, \frac{36769}{25080}, \frac{36769}{25080}, \frac{1502}{1045}, \frac{35369}{25080}, \frac{6767}{5016}, \frac{33133}{25080}, \frac{33133}{25080}$, $\frac{6767}{5016}, \frac{35369}{25080}, \frac{1502}{1045}, \frac{18767}{12540}, \frac{37859}{25080}, \frac{37859}{25080}, \frac{18767}{12540}, \frac{4588}{3135}, \frac{1502}{1045}, \frac{35369}{25080}, \frac{35369}{25080}, \frac{1502}{1045}, \frac{4588}{3135}, \frac{37859}{25080}, \frac{19219}{12540}, \frac{37859}{25080}, \frac{36769}{25080}, \frac{36769}{25080}$, $\frac{38503}{25080}, \frac{19027}{12540}, \frac{19027}{12540}, \frac{38503}{25080}, \frac{17}{11}$
Truncated Cube	$\frac{3}{4}, \frac{13}{12}, \frac{4}{3}, \frac{83}{60}, \frac{77}{60}, \frac{13}{12}, \frac{7}{12}, \frac{7}{12}, \frac{13}{12}, \frac{29}{20}, \frac{13}{10}, \frac{77}{60}, \frac{4}{3}, \frac{31}{20}, \frac{29}{20}, \frac{29}{20}, \frac{13}{10}, \frac{77}{60}, \frac{83}{60}, \frac{29}{20}, \frac{31}{20}, \frac{47}{30}, \frac{91}{60}$
Truncated Dodecahedron	$\frac{89}{150}, \frac{173}{150}, \frac{127}{90}, \frac{731}{450}, \frac{151}{90}, \frac{731}{450}, \frac{112}{75}, \frac{173}{150}, \frac{39}{50}, \frac{89}{150}, \frac{64}{45}, \frac{394}{225}, \frac{751}{450}, \frac{173}{150}, \frac{112}{75}, \frac{173}{150}, \frac{751}{450}, \frac{863}{450}, \frac{167}{90}, \frac{863}{450}, \frac{751}{450}, \frac{731}{450}, \frac{127}{90}, \frac{64}{45}, \frac{394}{225}, \frac{9}{5}, \frac{89}{45}, \frac{448}{225}$, $\frac{438}{225}, \frac{863}{450}, \frac{167}{90}, \frac{151}{90}, \frac{731}{450}, \frac{751}{450}, \frac{394}{225}, \frac{438}{225}, \frac{448}{225}, \frac{92}{45}, \frac{61}{30}, \frac{438}{225}, \frac{394}{225}, \frac{9}{5}, \frac{907}{450}, \frac{467}{225}, \frac{476}{225}, \frac{61}{30}, \frac{863}{450}, \frac{438}{225}, \frac{467}{225}, \frac{476}{225}, \frac{467}{225}, \frac{92}{45}, \frac{448}{225}, \frac{89}{45}, \frac{448}{225}$, $\frac{907}{450}, \frac{467}{225}, \frac{473}{225}, \frac{191}{90}$
Small Rhombicuboctahedron	$\frac{843}{1680}, \frac{51}{80}, \frac{843}{1680}, \frac{257}{420}, \frac{767}{1680}, \frac{767}{1680}, \frac{257}{420}, \frac{1133}{1680}, \frac{1229}{1680}, \frac{1229}{1680}, \frac{1133}{1680}, \frac{323}{420}, \frac{1229}{1680}, \frac{1133}{1680}, \frac{1133}{1680}, \frac{1229}{1680}, \frac{323}{420}, \frac{1343}{1680}, \frac{1343}{1680}, \frac{63}{80}, \frac{421}{560}, \frac{63}{80}, \frac{57}{70}$
Cuboctahedron	$\frac{11}{24}, \frac{7}{12}, \frac{11}{24}, \frac{11}{24}, \frac{11}{24}, \frac{5}{8}, \frac{5}{8}, \frac{7}{12}, \frac{5}{8}, \frac{2}{3}$
Icosidodecahedron	$\frac{29}{60}, \frac{61}{90}, \frac{61}{90}, \frac{29}{60}, \frac{29}{60}, \frac{29}{60}, \frac{127}{180}, \frac{7}{9}, \frac{127}{180}, \frac{7}{9}, \frac{127}{180}, \frac{61}{90}, \frac{61}{90}, \frac{127}{180}, \frac{7}{9}, \frac{49}{60}, \frac{38}{45}, \frac{38}{45}, \frac{49}{60}, \frac{157}{180}, \frac{49}{60}, \frac{7}{9}, \frac{49}{60}, \frac{157}{180}, \frac{157}{180}, \frac{38}{45}, \frac{38}{45}, \frac{157}{180}, \frac{8}{9}$

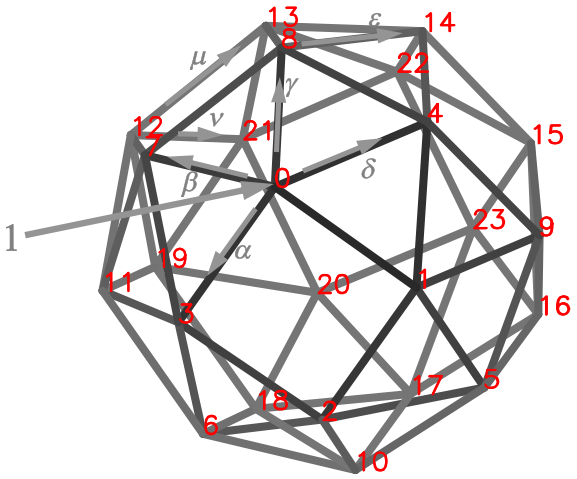


Fig. 6. Base van Steenwijk's current configuration in the Snub Cube (SC). Seven unknown currents α, β, γ, δ, ε, μ and ν are introduced. Equal currents of 1/23 are extracted from each node from 1 to 23 (not shown).

Corner theorem in Archimedean networks

Particular two-point resistances in AS networks are not related through the symmetries specific to the AS, but result from general theorems. This is the case of two-point resistances around a node with three legs (Fig. 10a), where one leg, from node 0 to node s, is in a plane of symmetry Π of the network, and the two other legs, from node 0 to nodes k and p, are symmetrical. One general theorem can be demonstrated (i.e. two + one legs corner theorem) [18], but, in the present case, the three legs are unity resistors and the simplified form can be used. This corner theorem states (Fig. 10a) that the base resistances R_{sk}=R_{sp} and R_{kp} are related to the leg resistances R_{0k}=R_{0p} and R_{0s} by [16]:

$$\begin{cases} R_{sk} = R_{sp} = R_{0k} + 2R_{0s} - 1 \\ R_{kp} = 4R_{0k} - R_{0s} - 1 \end{cases}. \tag{16}$$

In the AS (Fig. 1), nodes with multiplicity 3 carrying a plane of symmetry are found only in the truncated PS networks (TT, TO, TI, TC and TD). Nodes with multiplicity 3 in the GRCO and the GRCD networks (Fig. 2) do not carry any plane of symmetry.

When applying the corner theorem Eq. (16) to the TO (Fig. 10b), following the node numbering convention of Fig. 1, we have s=5, p=1 and k=3, and we get:

$$\begin{cases} R_{sk} = R_{sp} = R_{51} = R_{01} + 2R_{05} - 1 = \dfrac{625}{1008} + 2\dfrac{341}{504} - 1 = \dfrac{109}{112} \\ R_{kp} = R_{13} = 4R_{01} - R_{05} - 1 = 4\dfrac{625}{1008} - \dfrac{341}{504} - 1 = \dfrac{45}{56} \end{cases}, \tag{17}$$

using the expressions of Table 3 for R_{01} and R_{05}. The results of Eq. (17) from the corner theorem indeed coincide with the expressions of Table 3 for R_{51}=R_{06} and R_{13}=R_{02}.

Similarly, for the TI (Fig. 1), we have s=6, p=1 and k=4, and we get:

$$\begin{cases} R_{sk} = R_{sp} = R_{61} = R_{01} + 2R_{06} - 1 = \dfrac{16273}{25080} + 2\dfrac{8389}{12540} - 1 = \dfrac{24749}{25080} \\ R_{kp} = R_{14} = 4R_{01} - R_{06} - 1 = 4\dfrac{16273}{25080} - \dfrac{8389}{12540} - 1 = \dfrac{11617}{12540} \end{cases}, \tag{18}$$

using the expressions of Table 3 for R_{01} and R_{06}. The results of Eq. (18) from the corner theorem again coincide with the expressions of Table 3 for R_{61}=R_{07} and R_{14}=R_{03}. While it is not surprising that a general theorem is satisfied, it definitely provides a non-trivial check of the correctness of the obtained fractional expressions.

In the case of the truncated AS networks with a triangular face (TT, TC and TD), there is the additional property that R_{kp}=R_{0k}, and the corner theorem takes the form:

$$\begin{cases} R_{sk} = R_{sp} = R_{0k} + 2R_{0s} - 1 = \dfrac{7R_{0s} - 2}{3} \\ R_{kp} = R_{0k} = \dfrac{R_{0s} + 1}{3} \end{cases}. \tag{19}$$

Thus, in the case of the TD network (Fig. 10c), we have s=9, k=1 and p=10, which leads to:

$$\begin{cases} R_{sk} = R_{19} = \dfrac{7R_{09} - 2}{3} = \dfrac{1}{3}\left(7\dfrac{39}{50} - 2\right) = \dfrac{173}{150} \\ R_{kp} = R_{1,10} = \dfrac{R_{09} + 1}{3} = \dfrac{1}{3}\left(\dfrac{39}{50} + 1\right) = \dfrac{89}{150} \end{cases}, \tag{20}$$

using the result of Table 3 for R_{09}. Again, we obtain from the corner theorem the results of Table 3 for R_{19}=R_{02} and $R_{1,10}$=R_{01}. Similarly, for the TT, with the node numbering of Fig. 1, we have s=3, k=1 and p=2, and we obtain:

$$\begin{cases} R_{sk} = R_{13} = \dfrac{7R_{03} - 2}{3} = \dfrac{1}{3}\left(7\dfrac{7}{10} - 2\right) = \dfrac{29}{30} = R_{04} \\ R_{kp} = R_{01} = \dfrac{R_{03} + 1}{3} = \dfrac{1}{3}\left(\dfrac{7}{10} + 1\right) = \dfrac{17}{30} \end{cases}, \tag{21}$$

and for the TC, we have s=1, k=7 and p=8 (Fig. 1), and we obtain:

$$\begin{cases} R_{sk} = R_{17} = \dfrac{7R_{01} - 2}{3} = \dfrac{1}{3}\left(7\dfrac{3}{4} - 2\right) = \dfrac{13}{12} = R_{02} \\ R_{kp} = R_{78} = \dfrac{R_{01} + 1}{3} = \dfrac{1}{3}\left(\dfrac{3}{4} + 1\right) = \dfrac{7}{12} \end{cases}. \tag{22}$$

Relations between some two-point resistances in Archimedean and Platonic networks

Selected two-point resistances in AS networks can be related to resistances in PS networks. To establish a first set of relations, first, we prove a useful lemma. Consider one resistor a linking two nodes A and B in any resistor network (Fig. 11a), with an equivalent resistance R_{AB}. We are interested to express the resistance R_x between any two nodes between A and B along resistor a linked by a fraction x of a, hence the resistance between node A and a node X linked by the fraction x of the total resistor a (Fig. 11a). Let r be the equivalent resistance between A and B except for resistor a (Fig. 11b). We have R_{AB}=ar/(a+r), hence r=aR_{AB}/(a−R_{AB}). The resistance R_x corresponds to a resistor ax in parallel with a(1−x) in series with r (Fig. 11b), giving:

$$R_x = ax\frac{a(1-x) + r}{a + r} = ax(1-x) + x^2R_{AB}. \tag{23}$$

Now consider an AS network with triangles of resistors, such as the TT network (Fig. 11c). The triangle of resistors, a Δ configuration, can be replaced, using Kennelly's theorem (triangle-star or Δ-Y equivalence), by a Y configuration, namely adding a central node with three radial resistors from this central node, each having in this case a resistance of 1/3 [18]. After the addition of nodes (Fig. 11d), the TT network becomes a T network with equal resistors of value a=1/3+1+1/3=5/3. In the T network with edge unity, we have R_T=1/2 (Table 1). The resistance R_{03} in the TT network can be interpreted, using the lemma Eq. (23), as the resistance corresponding to a fraction x=3/5 of the closest neighbour resistance in the corresponding T network, which has R_{AB}=R_T×a=1/2×a, hence:

$$R_{03} = R_x = \frac{5}{3}\frac{3}{5}\left(1 - \frac{3}{5}\right) + \left(\frac{3}{5}\right)^2 R_T\frac{3}{5} = \frac{2 + 3R_T}{5} = \frac{7}{10}, \tag{24}$$

in agreement with the result in Table 3.

Table 4
Complete two-point resistances in the chiral Archimedean (AS) networks (Fig. 2) with edges carrying equal unity resistors. The given values correspond to the resistance between node 0 and node i, with increasing i from 1 to $V-1$ (see Table 2), with the convention in the numbering of nodes shown in Fig. 2.

AS Network	Two-point resistance values
Snub Cube	$\frac{15137}{38016}, \frac{1733}{3456}, \frac{15137}{38016}, \frac{14137}{38016}, \frac{20069}{38016}, \frac{20143}{38016}, \frac{1193}{3168}, \frac{14137}{38016}, \frac{401}{792}, \frac{21661}{38016}, \frac{18995}{38016}, \frac{20143}{38016}, \frac{20069}{38016}, \frac{18995}{38016}, \frac{21661}{38016}, \frac{613}{1056}, \frac{23171}{38016}, \frac{22691}{38016}, \frac{613}{1056}, \frac{1937}{3168}, \frac{2009}{3456}, \frac{21803}{38016}, \frac{2093}{3456}$
Snub Dodecahedron	$\frac{5964797}{14343240}, \frac{803629}{1406200}, \frac{803629}{1406200}, \frac{5964797}{14343240}, \frac{8984731}{23905400}, \frac{3435688}{8964525}, \frac{13627457}{23905400}, \frac{45182813}{71716200}, \frac{40564297}{71716200}, \frac{4778227}{8964525}$ $\frac{8984731}{23905400}, \frac{37376431}{71716200}, \frac{45660607}{71719200}, \frac{15326227}{23905400}, \frac{1892391}{2988175}, \frac{37376431}{71716200}, \frac{13627457}{23905400}, \frac{48175213}{71716200}, \frac{49914079}{71716200}, \frac{16952199}{23905400}$ $\frac{15326227}{23905400}, \frac{40564297}{71716200}, \frac{1892391}{2988175}, \frac{16895673}{23905400}, \frac{10521677}{14343240}, \frac{16895673}{23905400}, \frac{45660607}{71719200}, \frac{45182813}{71716200}, \frac{49914079}{71716200}, \frac{51341449}{71716200}$ $\frac{17517793}{23905400}, \frac{49240567}{71716200}, \frac{1774333}{2868648}, \frac{46559183}{71716200}, \frac{4163693}{5976350}, \frac{17752967}{23905400}, \frac{17586429}{23905400}, \frac{16319497}{23905400}, \frac{46559183}{71716200}, \frac{16319497}{23905400}$ $\frac{52281493}{71716200}, \frac{3190471}{4218600}, \frac{25868}{35155}, \frac{49240567}{71716200}, \frac{51341449}{71716200}, \frac{17752967}{23905400}, \frac{3668607}{4781080}, \frac{2726909}{3585810}, \frac{52281493}{71716200}, \frac{17517793}{23905400}$ $\frac{17586429}{23905400}, \frac{2726909}{3585810}, \frac{2213989}{2868648}, \frac{3190471}{4218600}, \frac{18008827}{23905400}, \frac{10697273}{14343240}, \frac{54360689}{71716200}, \frac{4614181}{5976350}, \frac{18394207}{23905400}$

Table 5
Complete two-point resistances in the Archimedean (AS) networks with three types of faces (Fig. 2) with edges carrying equal unity resistors. The given values correspond to the resistance between node 0 and node i, with increasing i from 1 to $V-1$ (see Table 2), with the convention for the numbering of nodes shown in Fig. 2.

Network	Two-point resistance values
GRCO	$\frac{5059}{7920}, \frac{36241}{34320}, \frac{11729}{9360}, \frac{3039}{2288}, \frac{130927}{102960}, \frac{36241}{34320}, \frac{18001}{25740}, \frac{2641}{2640}, \frac{63859}{102960}, \frac{1756}{2145}, \frac{127093}{102960}, \frac{45763}{34320}, \frac{11233}{7920}, \frac{3667}{2640}, \frac{29737}{25740}, \frac{22751}{20592}, \frac{2641}{2640}, \frac{29737}{25740}, \frac{1323}{1040}, \frac{30293}{20592}, \frac{51343}{34320}, \frac{147793}{102960}, \frac{978}{715}, \frac{30293}{20592}, \frac{1323}{1040}, \frac{127093}{102960}, \frac{45763}{34320}, \frac{3565}{2574}, \frac{17643}{11440}, \frac{1121}{720}, \frac{12937}{8580}, \frac{51343}{34320}, \frac{147793}{102960}, \frac{3667}{2640}, \frac{11233}{7920}, \frac{12937}{8580}, \frac{1121}{720}, \frac{54601}{34320}, \frac{1843}{1170}, \frac{279}{176}, \frac{158539}{102960}, \frac{51361}{34320}, \frac{151627}{102960}, \frac{3411}{2640}, \frac{158539}{102960}, \frac{13549}{8580}, \frac{1583}{990}$
SRCD	$\frac{60383}{114840}, \frac{83903}{114840}, \frac{83903}{114840}, \frac{60383}{114840}, \frac{18137}{28710}, \frac{52543}{114840}, \frac{52543}{114840}, \frac{18137}{28710}, \frac{81253}{114840}, \frac{18437}{22968}, \frac{31771}{114840}, \frac{31771}{114840}, \frac{18437}{22968}, \frac{81253}{114840}, \frac{24017}{28710}, \frac{18437}{22968}, \frac{81253}{114840}, \frac{81253}{114840}, \frac{18437}{22968}, \frac{24017}{28710}, \frac{104443}{114840}, \frac{35341}{38280}, \frac{35341}{38280}, \frac{104443}{114840}, \frac{35341}{38280}, \frac{31771}{114840}, \frac{31771}{114840}, \frac{35341}{38280}, \frac{22159}{22968}, \frac{36571}{38280}, \frac{33661}{38280}, \frac{635}{792}, \frac{33661}{38280}, \frac{36571}{38280}, \frac{113653}{114840}, \frac{113653}{114840}, \frac{22181}{22968}, \frac{13606}{14355}, \frac{103003}{114840}, \frac{33661}{38280}, \frac{33661}{38280}, \frac{103003}{114840}, \frac{13606}{14355}, \frac{22181}{22968}, \frac{14401}{14355}, \frac{116623}{114840}, \frac{116623}{114840}, \frac{14401}{14355}, \frac{113653}{114840}, \frac{22181}{22968}, \frac{36571}{38280}, \frac{36571}{38280}, \frac{22181}{22968}, \frac{113653}{114840}, \frac{115823}{114840}, \frac{113423}{114840}, \frac{113423}{114840}, \frac{115823}{114840}, \frac{651}{638}$
GRCD	$\frac{8687557}{13375719}, \frac{49184957}{44585730}, \frac{90492779}{66878595}, \frac{2251558}{1486191}, \frac{104481812}{66878595}, \frac{2251558}{1486191}, \frac{92387543}{66878595}, \frac{49184957}{44585730}, \frac{190646963}{267514380}, \frac{45395429}{44585730}, \frac{41543021}{66878595}, \frac{14779007}{17834292}, \frac{345148397}{267514380}, \frac{18145933}{12738780}, \frac{431484383}{267514380}$, $\frac{146254097}{89171460}, \frac{423905327}{267514380}, \frac{134600587}{89171460}, \frac{160336759}{133757190}, \frac{4431451}{3934035}, \frac{45395429}{44585730}, \frac{160336759}{133757190}, \frac{244867}{184620}, \frac{431615693}{267514380}, \frac{3303347}{1981588}, \frac{462416669}{267514380}, \frac{21817867}{12738780}, \frac{59070173}{38216340}, \frac{2889479}{1981588}, \frac{244867}{184620}$, $\frac{345148397}{267514380}, \frac{18145933}{12738780}, \frac{394156361}{267514380}, \frac{38614339}{22292865}, \frac{235148443}{133757190}, \frac{40487828}{22292865}, \frac{17276609}{9554085}, \frac{73688939}{44585730}, \frac{431615693}{267514380}, \frac{21817867}{12738780}, \frac{59070173}{38216340}, \frac{134600587}{89171460}, \frac{423905327}{267514380}, \frac{73688939}{44585730}, \frac{17276609}{9554085}$, $\frac{41425681}{22292865}, \frac{253470757}{133757190}, \frac{8379124}{4458573}, \frac{4146395}{2326212}, \frac{4507462}{2476985}, \frac{238017343}{133757190}, \frac{2133583}{1311345}, \frac{43031393}{26751438}, \frac{37285877}{22292865}, \frac{228744541}{133757190}, \frac{165850193}{89171460}, \frac{101077363}{53502876}, \frac{171858391}{89171460}, \frac{513097181}{267514380}, \frac{253470757}{133757190}$, $\frac{41425681}{22292865}, \frac{462416669}{267514380}, \frac{3303347}{1981588}, \frac{431484383}{267514380}, \frac{146254097}{89171460}, \frac{235148443}{133757190}, \frac{40487828}{22292865}, \frac{255591121}{133757190}, \frac{8582281}{4458573}, \frac{522228251}{267514380}, \frac{172170119}{89171460}, \frac{125772251}{66878595}, \frac{11396771}{6369390}, \frac{228744541}{133757190}, \frac{37285877}{22292865}$, $\frac{45643859}{26751438}, \frac{1876253}{1049076}, \frac{71294471}{38216340}, \frac{24621101}{12738780}, \frac{75728819}{38216340}, \frac{177238049}{89171460}, \frac{75004829}{38216340}, \frac{173631457}{89171460}, \frac{246541609}{133757190}, \frac{4507462}{2476985}, \frac{238017343}{133757190}, \frac{11396771}{6369390}, \frac{125772251}{66878595}, \frac{169773601}{89171460}, \frac{266677}{136836}$, $\frac{89514893}{44585730}, \frac{134588464}{66878595}, \frac{44436509}{22292865}, \frac{75728819}{38216340}, \frac{169773601}{89171460}, \frac{101077363}{53502876}, \frac{165850193}{89171460}, \frac{71294471}{38216340}, \frac{24621101}{12738780}, \frac{44436509}{22292865}, \frac{134588464}{66878595}, \frac{90299929}{44585730}, \frac{108024043}{53502876}, \frac{177238049}{89171460}, \frac{75004829}{38216340}$, $\frac{171858391}{89171460}, \frac{513097181}{267514380}, \frac{172170119}{89171460}, \frac{522228251}{267514380}, \frac{88112117}{44585730}, \frac{133887083}{66878595}, \frac{180091871}{89171460}, \frac{42815}{21114}, \frac{18028813}{8917146}, \frac{133887083}{66878595}, \frac{88267981}{44585730}, \frac{52378295}{26751438}, \frac{86951203}{44585730}, \frac{52378295}{26751438}$

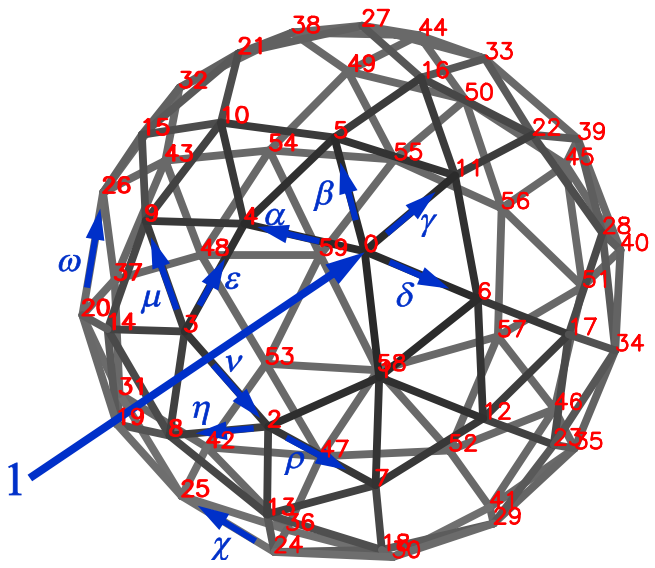


Fig. 7. Base van Steenwijk's current configuration in the Snub Dodecahedron (SD). Eleven unknown currents α, β, γ, δ, ε, μ, ν, η, ρ, ω and χ are introduced. Equal currents of 1/59 are extracted from each node from 1 to 59 (not shown).

The same reasoning can be applied to the resistance R_{TX} between triangles of any truncated AS network with triangles (TT, TC and TD) and related to the closest neighbour resistance R_X in the corresponding PS network, giving:

$$R_{TX} = \frac{2 + 3R_X}{5}. \tag{25}$$

Applying Eq. (25) to the TC (Fig. 1), we obtain, using R_C from Table 1:

$$R_{TC} = R_{01} = \frac{2 + 3R_C}{5} = \frac{1}{5}\left(2 + 3\frac{7}{12}\right) = \frac{3}{4}, \tag{26}$$

and for the TD:

$$R_{TD} = R_{09} = \frac{2 + 3R_D}{5} = \frac{1}{5}\left(2 + 3\frac{19}{30}\right) = \frac{39}{50}, \tag{27}$$

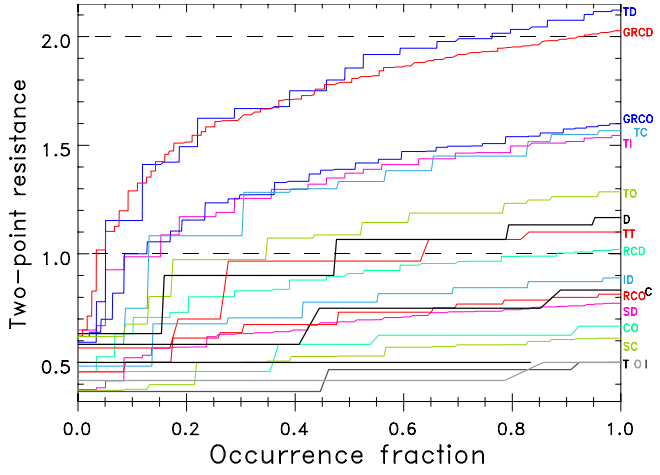


Fig. 8. Summary of two-point resistances between nodes of Perfect Solid (PS) and Archimedean Solid (AS) networks (Tables 3 to 5). For each network, as labelled using the conventions of Tables 1 and 2, the values of two-point resistances are arranged in increasing order, and presented as a function of their occurrence fraction, defined as the rank, with identical values repeated, divided by the total number of pairs in this network (see text).

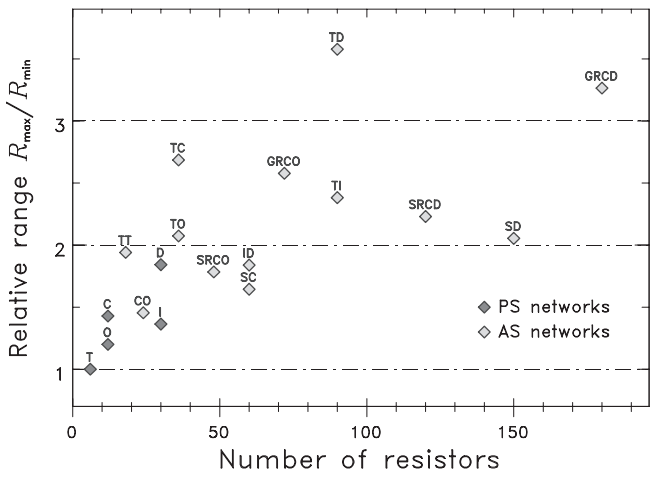


Fig. 9. Relative range R_{max}/R_{min} as a function of the number of resistors in PS and AS networks.

in agreement with the values in Table 3.

Finally, the Δ-Y transform can be applied to the triangles in the ID network (Fig. 11e). The obtained network becomes a D network with resistance 2/3. However, in this case, the referenced nodes are located in the middle of the resistors of the D network (Fig. 11f). Thus, we can state that the two-point resistances between the middle points of a D network with unity resistors (Fig. 11f) are the two-point resistances of the ID network with resistor 3/2.

Similarly, the two-point resistances between the middle points of the I network with unity resistors are the two-point resistances of the ID network with resistor 3/2, and the two-point resistances of the middle points of the C network are the two-point resistances of the CO network with resistor 3/2. As for the two-point resistances between the middle points of the T network, they are the two-point resistances of the O network with resistor 3/2. Thus, AS and PS networks are related and some AS networks emerge as the solution of particular problems concerning the PS networks.

Conclusions

In this paper, using VSM, we have established exact expressions for all two-point resistances in the complete set of the thirteen AS networks. These expressions are useful to check the accuracy of particular numerical or theoretical models based on other methods, such as Laplacian matrix [15] or Green functions [10–12]. The obtained values of the two-point resistances in AS networks cover a large range of values and they are widely different for the various AS networks, even for similar numbers of resistors in the network. For example, the maximum resistance in the TD network is 37% larger than the maximum resistance in the TI network, while both networks have 90 resistors.

These two-point resistances in AS networks, where consequences of symmetries can also be illustrated, provide a useful base knowledge when evaluating the capacity of AS networks to represent experimental situations. This is particularly true for current solid-state physics research when approaching novel compounds. New materials, for example fullerene [3–4] or faujacite mineral assemblies in zeolites [21–23], are found in nature or are completely artificial, such as synthetic graphene and other carbon nanocomposites [5–7]. In general, the properties of three-dimensional networks, which can be investigated using numerical codes, benefit greatly from theoretical approaches where the various symmetries of the considered networks are considered from the beginning. When elaborating a model to account for experimental data, it is also important to be aware of existing relations between two-point resistances in a given network or between different networks.

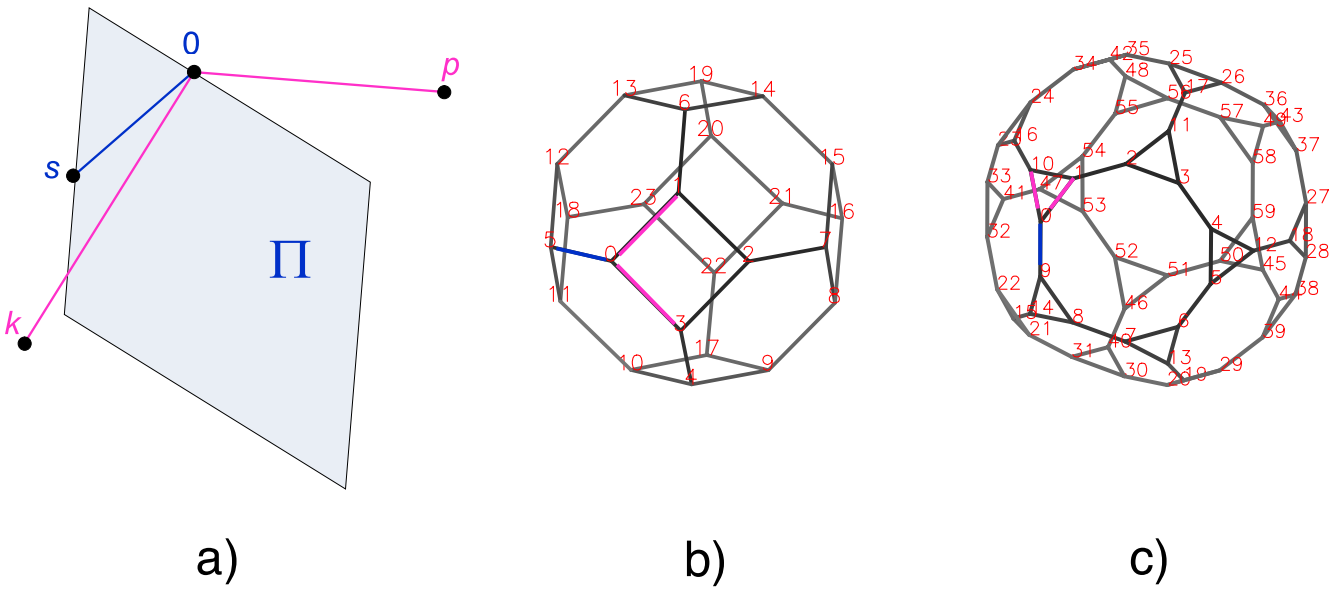


Fig. 10. a) Node configuration for the two + one legs corner theorem [18]. b) Application of the two + one legs corner theorem in the TO network. c) Application of the two + one legs corner theorem in the TD network.

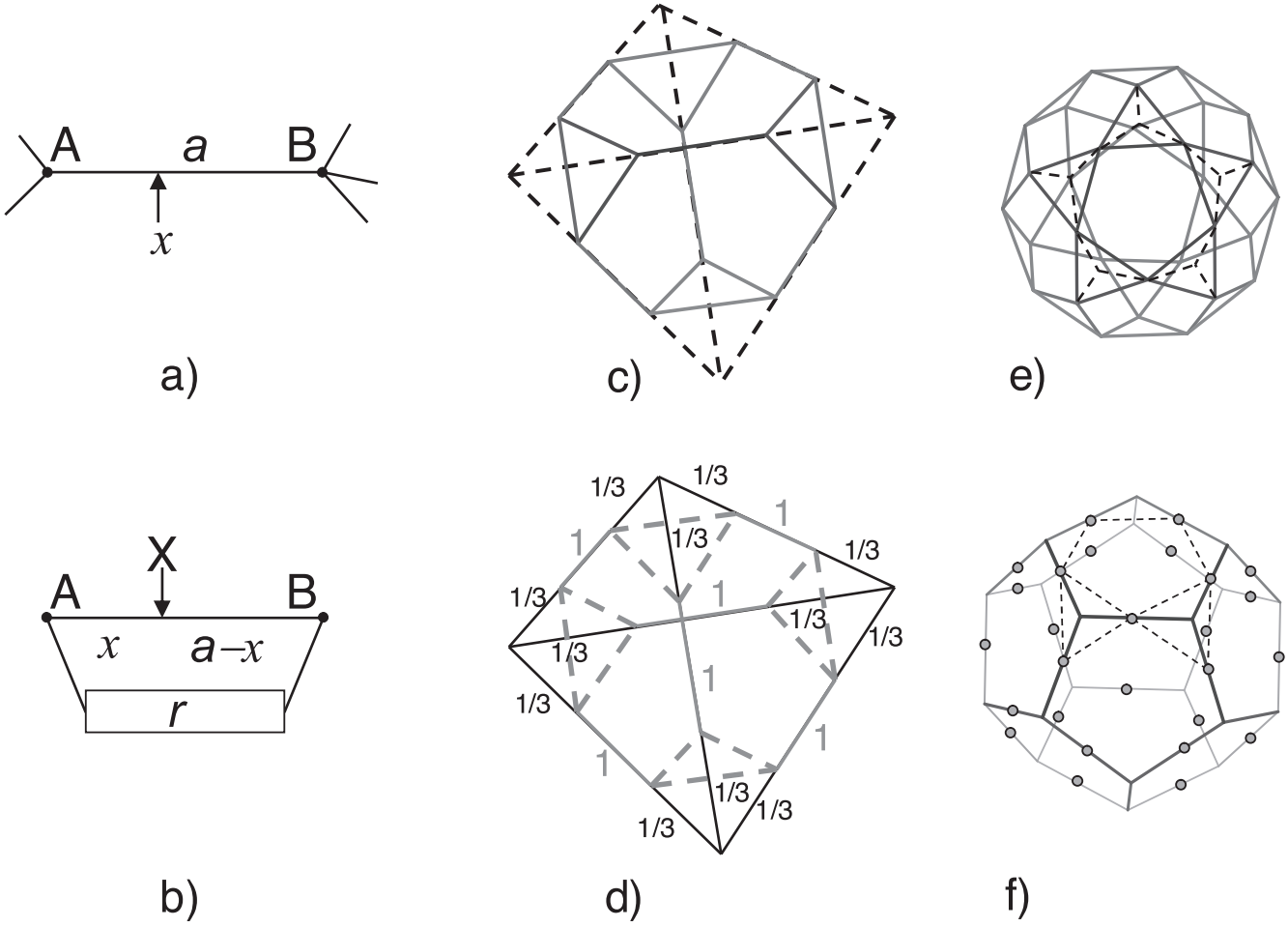


Fig. 11. a) Resistance along a fraction × of a resistor *a* in any network; b) Equivalent diagram to calculate the resistance across a fraction × of resistor *a*; c) Application of Kennelly's Δ to Y transform to the triangles of the TT network; d) Result of the application of Kennelly's Δ to Y transform to the triangles of the TT network; e) Application of Kennelly's Δ to Y transform to the triangles of the ID network. For clarity, the transform is illustrated only with selected triangles. f) ID network of the middle points in the D network.

Resistor networks still remain fascinating objects of investigations, and even complex three-dimensional networks can be analysed using fundamental theorems or elementary general methods. Establishing two-point resistances reveals properties that can be translated to numerous other applications of the considered network. AS networks, in particular, offer numerous possibilities, as generic three-dimensional symmetrical networks, for example to develop novel decision processes based on neural networks [30]. Indeed, the particular connectivity pattern of AS networks can provide interesting topological structures for decision algorithms. In general, AS networks open perspectives in network design and expand further the capacity of networks to represent adequate and efficient models of complexity in all fields of science [31,32].

Declaration of Competing Interest

The authors declare that they have no known competing financial interests or personal relationships that could have appeared to influence the work reported in this paper.

Acknowledgement

We thank two anonymous reviewers for their positive comments. This work contributes to the IdEx Université de Paris *ANR-18-IDEX-0001*.

References

[1] Kirchhoff G. Über die Auflösung der Gleichungen, auf welche man bei der Untersuchung der linearen Vertheilungen galvanischer Ströme geführt wird. Ann Phys Chem 1847;72:497–508.
[2] Kennelly AE. 1899 Equivalence of triangles and three-pointed stars in conducting networks. Electric World Engin 1899;34:413–4.
[3] Kroto HW, Heath JR, O'Brien SC, Curl RF, Smalley RE. Buckminsterfullerene Nature 1985;318:162–3.
[4] Kroto H. Symmetry, space, stars and C-60. Rev Mod Phys 1997;69:703–22.
[5] Geim AK, Novoselov KS. The rise of graphene. Nat Mater 2007;6(3):183–91.
[6] Geim AK. Graphene prehistory. Phys Scr 2012;146:014003.
[7] Yu HD, Heider S, Advani A. 3D microstructure based network model for the electrical resistivity of unidirectional carbon composites. Compos Struct 2015;134:740–9.
[8] van Steenwijk FJ. Equivalent resistors of polyhedral resistive structures. Am J Phys 1998;66(1):90–1.
[9] Moody J, Aravind PK. Resistor networks based in symmetrical polytopes. Electron J Graph Theor App 2015;3:56–69.
[10] Owaidat MQ. Regular resistor lattice networks in two dimensions (Archimedean lattices). Appl Phys Res 2014;6:100–8.
[11] Asad JH, Diab AA, Owaidat MQ, Hijjawi RS. Khalifeh JM Infinite body centered cubic network of identical resistors. Acta Phys Polon 2014;125:60–4.
[12] Mamode M. Electrical resistance between pairs of vertices of a conducting cube and continuum limit for a cubic resistor network. J Phys Comm 2017;1(3):035002. https://doi.org/10.1088/2399-6528/aa8ab6.
[13] Tan Z-Z, Essam JW, Wu FY. Two-point resistance of a resistor network embedded on a globe. Phys Rev E 2014;90:012130.
[14] Tan Z, Tan Z-Z. Potential formula of an m×n globe network and its application. Sci Rep 2018;8:9937.
[15] Tan Z-Z. The basic principle of m×n resistor network. Commun Theor Phys 2020;7:055001.
[16] Perrier F, Girault F. An example of the relevance of symmetry in physics: Corner theorems in grids and cubic resistor networks. Eur J Phys 2020;41:035805.
[17] Perrier F, Girault F. Rotational invariance in resistor networks: Two-point resistances around an *n*-fold corner. Eur J Phys 2021;42:025803.
[18] Perrier F, Girault F. Recurrence relations in m×3 scaffolding and globe resistor networks. Phys Scr 2021;96:085003.
[19] Perrier F, Girault F. Symmetries, recurrence and explicit expressions of two-point resistances in 2×n globe resistor networks. Eur J Phys 2021;42:055201.
[20] Kepler J. Harmonices Mundi. Ed Johann Planck 1619.
[21] Torquato S, Jiao Y. Dense packings of the Platonic and Archimedean solids. Nature 2009;460(7257):876–9.
[22] Damasceno PF, Engel M, Glotzer SC. Predictive self-assembly of polyhedra into complex structures. Science 2012;337(6093):453–7.
[23] Peuronen A, Lehtimäki E, Lahtinen M. Self-assembly of water-mediated supramolecular cationic Archimedean solids. Cryst Growth Des 2013;13(10):4615–22.
[24] Kubala P. Random sequential adsorption of Platonic and Archimedean solids. Phys Rev E 2019;100(4). https://doi.org/10.1103/PhysRevE.100.042903.
[25] Schwerdtfeger P, Wirz LN, Avery J. The topology of fullerenes. Comput Mol Sci 2015;5:96–145.
[26] Ferdov S. Conventional synthesis of layer-like zeolites with faujacite (FAU) structure and their pathway of crystallisation. Micropor Mesopor Mat 2020;303:110263.
[27] Coxeter HSM. Regular Polytopes. New York: Dover Publications; 1963.
[28] Datta B, Maity D. Platonic solids, Archimedean solids and semi-equivelar maps on the sphere. Discr Math 2022;345:112652.
[29] Batle J, Shotov AV, Maleev AV. Dipole-dipole minimum energy configuration for Platonic, Archimedean and Catalan solid structures. Phys Lett A 2020;384:126916.
[30] Denby B. Neural networks in high energy physics. Comp Phys Comm 1999;119:219–31.
[31] Strogatz SH Exploring complex networks. Nature 2001; 410:268-27.
[32] Ghil M. A century of nonlinearity in the geosciences. Earth Space Sci 2019;6(7):1007–42.